HHS Public Access

Author manuscript

Brachytherapy. Author manuscript; available in PMC 2021 November 01.

Published in final edited form as:

Brachytherapy. 2020 ; 19(6): 767–776. doi:10.1016/j.brachy.2020.07.013.

Multi-Material 3D Printing in Brachytherapy: Prototyping Teaching Tools for Interstitial and Intracavitary Procedures in Cervical Cancers

Sabrina Campelo[1], **Ergys Subashi, PhD**[2], **Sheridan G. Meltsner, PhD**[3], **Zheng Chang, PhD**[3], **Junzo Chino, MD**[3], **Oana Craciunescu, PhD**[3,*]

[1]Medical Physics Graduate Program, Duke University, 2424 Erwin Rd, Durham, NC 27705, USA.

[2]Department of Medical Physics, Memorial Sloan Kettering Cancer Center, New York, NY, USA

[3]Department of Radiation Oncology, Duke University Medical Center, 20 Duke Medicine Circle, Durham, NC 27710, USA.

Abstract

Purpose: As the utilization of brachytherapy procedures continues to decline in clinics, a need for accessible training tools is required to help bridge the gap between resident comfort in brachytherapy training and clinical practice. To improve the quality of intracavitary and interstitial HDR brachytherapy education, a multi-material modular 3D printed pelvic phantom prototype simulating normal and cervix pathological conditions has been developed.

Methods and Materials: Patient anatomy was derived from pelvic CT and MRI scans from 50 representative patients diagnosed with localized cervical cancer. Dimensions measured from patients' uterine body and uterine canal sizes were used to construct a variety of uteri based off of the averages and standard deviations of the subjects in our study. Soft-tissue anatomy was 3D printed using Agilus blends (shore 30 and 70), and modular components in Vero (shore 85).

Results: The kit consists of four uteri, a standard bladder, standard rectum, two embedded GTVs and four clip-on GTV attachments. The three anteverted uteri in the kit are based on the smallest, the average, and the largest dimensions from our patient set while the retroverted uterus assumes average dimensions.

Conclusions: This educational HDR gynecological pelvic phantom is an accessible and cost-effective way to improve radiation oncology resident training in intracavitary/interstitial brachytherapy cases. Implementation of this phantom in resident education will allow for more thorough and comprehensive physician training through its ability to transform the patient

*Corresponding Author: Oana Craciunescu: oana.craciunescu@duke.edu.

Disclosure

S.C, O.C, E.S, and J.C have a patent pending on the device discussed in this article.

Developed by Duke University Medical Physics Graduate Program, Duke University.

To make use of project files and documents, please contact the Duke University Medical Physics Graduate Program.

scenario. It is expected that this tool will help improve confidence and efficiency when performing brachytherapy procedures in patients.

Keywords

Brachytherapy; 3D printing; cervical cancer; pelvic phantom; resident training; gynecological malignancies

Introduction

The utilization of brachytherapy practice has been declining over the years. The decline has been linked to a variety of factors including a lack of training opportunities[1,2]. A recent initiative set forward by the American Brachytherapy Society calls to address this decline by implementing the “300 in 10 Strategy” in which they hope to train 30 competent brachytherapists per year over the course of 10 years[1]. Current requirements for graduates of a radiation oncology residency require residents to perform only seven cases of interstitial implants and 15 cases of intracavitary procedures during the course of their training[3]. A 2019 questionnaire sent to US radiation oncology residents in the Association of Residents in Radiation Oncology showed that confidence in brachytherapy practice had a rate of 54%, low compared to a staggering rate of 97% in SBRT/SRS procedures. The survey also presented a significant relationship between increased number of brachytherapy cases performed and increased confidence rate for starting brachytherapy practice[4].

Residents perform much of their brachytherapy training on live patients during their medical rotations. For a variety of factors including a finite amount of hands on training opportunities during patient procedures and a finite amount of time allocated in the brachytherapy rotation, radiation oncology residents may rely on phantoms for further training outside of patient exposure.

Current pelvic phantoms on the market are an expensive investment, making them less accessible. Many existing phantoms are made from rigid materials not representative of true anatomical material characteristics and lack modular components, resulting in repetitive non-comprehensive training[5]. Within gynecological brachytherapy procedures, anatomical differences in uteri, cervixes, and treatment volumes are unique to each patient. These mono-situational devices do not allow for training to comprehensively consider the variations encountered in human anatomy. This limitation may be overcome with the use of low-cost 3D printed components.

3D PolyJet printing opens up the possibility of fusing together complex polymers into a single multi-material print[6]. Multi-material PolyJet printing has found great use in the medical field, allowing for intricate and accurate fusing of different material components to be combined into one[7,8]. This has allowed for the creation of a variety of prototypes with intricate shapes and delicate details to be easily and affordably achieved[9]. This premium printing allows for the user to designate both the materials used and their range of hardness (shore durometer values).

Brachytherapy has begun utilizing 3D printing in applications such as printing custom skin[10] and vaginal[9] applicators for HDR procedures, printing negative molds of anatomy to be filled with gelatin to create needle insertion and suturing phantoms[11], and printing custom shielding designs[9].

The aim of this study is to improve the quality of intracavitary brachytherapy education by developing a modular 3D printed high-dose-rate (HDR) brachytherapy pelvic training phantom for training radiation oncology residents in tandem and ovoid and interstitial needle insertions for treating gynecological malignancies. Modularity allows for easy simulation of different stages of disease, allowing for a more thorough and comprehensive training for medical residents before having to perform such a procedure on a patient. Connecting different printed components allows for the ability to easily transform the patient's medical scenario presented. The stereolithography (STL) files needed to independently manufacture these tools are accessible to the medical community upon request for training and educational purposes. Additionally, this tool may be used by practicing radiation oncologists to refresh skills on less common complex cases.

By designing a modular multi-material 3D printed phantom for brachytherapy training based on patient anatomical data, we hope to overcome the characteristics that make existing phantoms less suitable for comprehensive training. With access to a more suitable training tool, we aim to help combat the decline in number of brachytherapy procedures performed in clinics.

Materials and Methods

Patient Dimensional Study

To create specifications for our 3D modeled uterine and HR-CTV dimensions, 50 patients with locally advanced cervical cancer were retrospectively analyzed. Patient anatomy was derived from pelvic CT and MRI scans from different representative patients who had been diagnosed with advanced stage localized cervical cancer. All patients met the following criteria: (1) have pathologically confirmed cervical cancer, (2) over the age of 18, (3) had been treated with radiation therapy with curative intent, (4) were treated between January 1st of 2009 and December 19th of 2018. Patients with distant metastatic disease were not included in the study.

HDR image guided adaptive brachytherapy (IGABT) for cervical cancer was performed in the Radiation Oncology Department at Duke University Cancer Center (Durham, NC) using the IGABT ESTRO and ABS[12–14] guidelines. IGABT implementation used a combination of imaging modalities including ultrasound guidance for tandem based applicator insertion, followed by CT for applicator delineation, and MRI for HR-CTV and normal tissue delineation. HR-CTV delineation is essential for the accurate placement and planning of complex intracavitary/interstitial implants[12].

Prior to IGABT, an MRI was performed to assess tumor regression and location post external beam radiation therapy (pbMRI). For each of the brachytherapy fractions, the same MRI sequence used for the pbMRI was used for planning purposes. All scans were acquired

on a Siemens 3T scanner (MAGNETOM Skyra, Siemens Healthcare, Germany). An axial T1 weighted 3D spoiled gradient recalled sequence was initially acquired (FOV = 30 cm, 0.9×0.9 mm isotropic in-plane voxel size, 1.0 mm slice thickness, TR = 3.7 ms, TE = 1.33 ms, Flip angle = 10.0 deg) and used for the registration with CT images. CT images were acquired on an Airo® Mobile CT scanner (MobiCT-32, Mobius Imaging, Phoenix Park 2 Shirley, Ma) with 1mm slice thickness and metal artifact reduction correction. An axial T2 weighted (pbMRI) 3D sequence was performed for HR-CTV delineation (FOV = 30 cm, 0.9×0.9 mm isotropic in-plane voxel size, 3.0mm slice thickness, TR = 2000 ms, TE = 121 ms). The T2-weighted sequence was used for target and normal tissue delineation.

Dimensions of patients' uterine canal sizes and uterine body sizes were measured and used to construct a variety of uteri based off of the averages and standard deviations of the subjects in our study. The measurements were conducted in the treatment planning software (TPS) (Eclipse v. 15.5, Varian Corp, Palo Alto, CA).

Measurements of the uterine bodies were performed on the T2 weighted brachytherapy MR images. The length of the uterine body was measured from the top of the cervix to the fundus. The width was measured both across the top of the cervix and across the midpoint between the cervix and the fundus perpendicular to the uterine canal.

Measurements of the uterine canal were performed on CT images. Canal measurements were performed one slice over from where high Hounsfield value voxels of the tandem were detected allowing for clear visualization of the low Hounsfield value voxels created by the airgap from the tandem. The full length of the uterine canal and the width of the canal above the cervix was measured. To measure the angle of the uterine canal, the image was oriented so the base of the measure angle tool was placed parallel to the flange, and the leg of the tool ran along the entrance of the canal.

HR-CTV Volume and Location Study

HR-CTV volumes and locations were recorded from the pre brachy T2 weighted MRI images in the TPS for each of the 50 patients included in the study. Volumes of the HR-CTVs were recorded from the contours using tools in the TPS. The location study was performed through visualization of patient scans and HR-CTV contours superimposed on the scan, and by determining the depth the HR-CTV penetrated into the uterine and cervical bodies. For this purpose, the uterus was divided in three areas: lower, middle, upper.

3D Modeling

Patient anatomy was derived from an anonymized average patient pelvic CT scan. Open source software, 3D Slicer (Slicer 4.10.1), was used to import and convert contoured DICOM data into 3D model STL files. Organs of interest for our prototype include the vaginal canal and uterus. A standard rectum and bladder were also printed. Individual STL files from a single patient were exported from 3D Slicer and imported into Shapr3D (Shapr3D zrt, 3.35.0, Hungary). This computer aided design (CAD) software allows for the manipulation of already existent STL files, as well as the creation of new designs created from a series of sketches which are further manipulated to include more representative features such as hollowed out cavities and canals.

Results from the patient dimensional study were used to construct the 3D uterine bodies in CAD software.

Existent STL files exported from 3D Slicer were used as a baseline to create a smoother and more consistent STL model. Dimensions derived from results of the patient study were drawn superimposed on the imported STL file in the CAD software. The STL of the uterine body was used as a general guideline to construct the shape of the uterine sketch while maintaining the desired dimensions as determined from the patient study (Figure 1).

The new sketch was extracted from the 2D sketch plane into the 3D body plane to encompass the width of the STL uterus body. Lateral edges of the new body were shaped by the use of a Boolean subtraction operator allowing for the subtraction of overlapping STL bodies with intersecting points. A new body was sketched and extracted to be used as the subtracting body to our newly extracted uterus.

A 2D sketch of the uterine canal was sketched superimposed on the patient CT scan using results from the patient dimensional study. The uterine canal was assumed to have a uniform cylindrical nature. The sketch was extracted to a height equal to the width of the uterine canal into the 3D plane. The uterine canal body was then placed into the center of the uterus and a Boolean operation was performed subtracting the uterine canal from the uterus resulting in an open cavity.

The vaginal canal was designed using ellipsoids based on speculum dimensions (KleenSpec® 590 Series, Figure 2)[15]. Construction of the canal was designed to support the insertion and opening of the speculum while still providing vaginal wall tension during the expansion.

Dimension F was used to determine the length of the vaginal canal and dimension B was used to construct the lateral width of the canal on the minor axis of the ellipse. E_2 was used to calculate the opening of the vaginal canal and E_1 was used to construct the end height of the canal before reaching the cervical entrance. To ensure a secure closing between the canal and uterus, an additional endpoint ellipse was added to ensure the vaginal canal descended to the height of the uterus directly past the cervix (Figure 2b).

The three ellipses above were combined using the loft extrusion feature, creating a smooth connection between the sketches resulting in a singular new 3D component.

Internal GTVs

For the purpose of this study, phantom GTV volumes were designed for the training phantom based off results from the volume and location of the HR-CTV analysis from the patient study. Based on ICRU 89[16], the HR-CTV is defined as the volume encapsulating the cervix, residual GTV, and residual pathologic tissue. Subsequently, we used HR-CTV contours to define these phantom GTVs in order to implement a physical tumor volume, represented by differently colored printed material within the phantom cervix/uterus, and allow for direct feedback for evaluating trainee needle placement.

External GTVs

Four external GTVs were designed based off of volume analysis conducted in the patient study. Because of the wide variations in the HR-CTV contours, the external clip-ons were designed to be equal to the minimum, mean, medium, and maximum volumes reported in the volume study.

Design of Outer Casing

The outer case was designed to hold all anatomical components in place while also serving as a closed cavity representing the human body. The non-anthropomorphic outer box design was most favorable given its simplicity, low production cost, and no need for post processing. The box was created by extracting two rectangles which encompassed the entirety of the organ components arranged in their connected form.

Supports were extracted from the bottom of the box to hold the canal, uterus, and rectum in place. This was accomplished by extracting simple rectangles encompassing the floating dimensions of the vagina and rectum, and then performing a Boolean subtraction to create form-fitting cutouts to act as supports for the bodies.

Modularity Design

The modular components of this training kit allow for different anatomical features to be easily interchanged to transform the patient scenario. A simple peg design was successfully utilized in terms of its discrete and compact design allowing for a clean blend into the anatomical components. This design requires the male pegs be printed in rigid materials (Vero, Stratasys) while the female canals be printed in a flexible material (Agilus30, Stratasys). The natural friction of the rigid material against the rubber-like surface holds the two components in place.

Shore Value Determination

Shore durometer values, which determine the rigidity of a given material, were assigned to each anatomical component in the phantom to represent appropriate levels of flexibility based on known anatomical Young's modulus of elasticity values[17].

Vero Clear material was assigned to rigid components including modularity connections and the outer case. Agilus30 was assigned to more flexible components including the vaginal canal, uterus, rectum, and bladder. Each component was assigned a shore value ranging from 30–80 to further individualize the levels of flexibility.

To assign representative shore values to each individual organ component in our prototype, an equation reported into British Standards[18,19] which evaluates the relationship between Young's modulus and shore hardness was used (Equation 1):

$$S_H = 100\, erf\left(3.186 * 10^{-4}\sqrt{E}\right)$$

where S_H represents the shore value on the A durometer scale, erf represents the error function, and E represents Young's modulus in units of Pascals. Experimental test data from

Baah-Dwomoh[20] determined the qualities of Young's modulus properties for our tissues of interest including the uterus, vagina, bladder, and rectum.

3D Printing

All finalized designs were printed on the Stratasys J750 PolyJet printer using the software GrabCad (Stratasys, Cambridge, MA). This printer is capable of multi-material photopolymer printing allowing for designation of shore value selection and filament color selection. It prints on the resolution of 42/42/14 (h/l/w) microns and carries a build plate dimension of 490×390×200mm. The printer supports water and alcohol soluble support materials which require prints to go through post processing while they are done. Finalized prints are submerged in 99% Isopropyl Alcohol until support materials are dissolved and washed off with a waterjet allowing for smooth finish of cavity prints.

Results

Patient dimensional study

The results of the patient uterus dimensional study and the HR-CTV volume study (Table 1) were used to construct four model uteri and six total GTVs.

Three anteverted uteri were designed based on the smallest, the average, and the largest dimensions from our patient set: Uterine body length (7.87 ± 2.06 cm), body width at top of cervix (2.784 ± 0.71 cm), body width at uterine midpoint (4.45 ± 1.29cm), canal length (6.23 ± 1.39 cm), canal angle (27.6° ± 8.49°). The fourth uterus is retroverted and uses average dimensions. The dimensions used to construct the four uteri are presented in Table 2.

HR-CTV Volume and Location Study

The HR-CTV location study was used to capture where the embedded GTVs would be positioned within the uterine bodies. The embedded GTVs are more representative of local cervical cancer with extension into the lateral paracervical tissues (stages IIB and IIIB), commonly treated with brachytherapy. The location study also gave insight as to where GTV connection channels should be placed. From the study, it was evident that contoured HR-CTV volumes were most commonly present in the lower sector outside the uterus and cervix and less commonly infiltrated the upper third of the uterine body (Figure 3; Figure 4). HR-CTV volumes were based on 29.06 ± 18.53ml results.

Shore Value Calculation Results

Young's modulus values were determined from previously published literature. Equation 1 was used to calculate shore A values presented in Table 3.

3D Modeling

The resultant uterine body is shown in Figure 5D. The canal was created as shown in Figure 6.

The box resulted in an 18.5×13×12.5 cm (l/w/h) rectangle. The front of the box included an ellipsoid cut-out for the vaginal opening. Two groves were created on the sides of the vaginal cut-out allowing for pegs attached to the side of the vagina to securely slide in place. The anatomy support structures are shown in Figure 7.The diameters of the ellipsoids used to construct the vaginal canal are listed in Table 4. Components were successfully connected through peg style modular clips (Figure 8).

Final 3D Model Design

The final design of the training phantom (Figure 9) includes the following STL files:

A. 1x Outer Case
B. 3x Anteverted Uteruses *
C. 1x Retroverted Uterus
D. 4x External GTVs
E. 1x Vaginal Canal
F. 1x Rectum
G. 1x Bladder

* 2 embedded GTVs in the small and large uterus

Printed Training Kit

The final kit (Figure 10) was printed on the Stratasys J750 printer at the Duke University Innovation Co-Lab (Durham, NC). Final shore values assigned for printing are listed in Table 5.

Material Costs

The cost of materials to manufacture the kit is approximately $631. This was determined based on material prices per gram reported between December 2019-March 2020. The full model results in 2,869 grams of material and approximately 1,935 grams of support material. The amount of support material required is dependent on how the model is placed on the digital print bed when sending to the printer.

This cost is based on a series of quotes which shows an average price for the component materials (Agilus and Vero) to be about $178 per kg, and the average price for the support material (FullCure 705) to be about $62.50 per kg.

Primary Materials: 2, 869 g × $ 178/kg = $ 510.00
Support Materials: 1, 935 g × $ 62.50/kg = $ 120.94
Total cost of materials: $ 630.94

Discussion

This work aims to demonstrate the feasibility of using patient CT/MRI data to design and manufacture complex 3D printed anatomical structures. The designed phantom training kit accurately represents the critical anatomical structures for practicing tandem based

brachytherapy procedures. While other 3D printed brachytherapy phantoms exist[10,11], our presented 3D printed kit exhibits four major advantages over existing phantoms in that: (1) It incorporates flexible materials which accurately mimic human tissue properties, (2) the phantom can be entirely and directly printed without the use of molds and external materials (3) printing the uterus in clear materials allows for the physician to check resident performance of tandem and needle insertions without needing access to a medical imaging scanner, and (4) the cost for manufacturing the full kit is significantly less than most existent training phantoms on the current market, making this an ideal option when selecting training tools. For smaller clinics and institutions not housing their own PolyJet printer, a variety of additive manufacturing companies including Stratasys and Proto3000 provide services to print STL files submitted through their servers.

Results from the patient dimensional study suggests there is a benefit to having a kit that simulates the variances in human anatomy that one might encounter from patient to patient while performing tandem based brachytherapy procedures. The training kit accommodates the insertion of one tandem and two ovoids. In order to incorporate muscular tension and a snug fit of the speculum traveling through the vaginal canal, medium and large speculum dimensions were averaged to design the canal.

The FDA does not regulate training devices not used in the operating room therefore eliminating the need for following strict biocompatibility and sterilization regulations in our training phantom.

Limitations of the shore value flexibilities exist. Of the materials compatible with our PolyJet printer, Agilus30 provides the lowest available shore value of 30. As specified in Table 3, shore values under 30 were calculated, but cannot be physically performed. In these cases, the lowest shore value of Agilus30 is used. However, a relationship between sample thickness and material elongation exists[21,22]. Thinner samples are capable of greater flexibility and larger elongation values. This limitation was addressed by using thinner walls to construct the organ anatomy.

An evaluation study will be performed by physician residents and judged by an attending consisting of both visual verification of applicator and needle placement, as well as verification by CT imaging. A future prototype of the kit will incorporate uterine bodies which are compatible with existent manufactured gynecological pelvic phantoms such as the EVA Gynecologic Mannequin (Simulaids, Saugerties, NY).

Conclusion

We have developed a modular pelvic phantom with detachable anatomical components allowing for more thorough and comprehensive training for medical residents. We foresee that by having created an accessible and low-cost training phantom, we can help improve resident comfort in performing these procedures and contribute to the American Brachytherapy Society call for 30 new brachytherapists per year for 10 years.

Acknowledgements

This work was funded by the Duke University Innovation Co-Lab.

References

1. Harari PM. Brachytherapy: Call to arms. Brachytherapy Take it forward Am Soc Radiat Oncol Mag. 2019:5. www.astro.org.
2. Compton JJ, Gaspar LE, Shrieve DC, et al. Resident-reported brachytherapy experience in ACGME-accredited radiation oncology training programs. Brachytherapy. 2013. doi:10.1016/j.brachy.2013.06.004
3. ACGME. ACGME Program Requirements for Graduate Medical Education in Radiatoin Oncology. ACGME Website. 2019:1–7.
4. Marcrom SR, Kahn JM, Colbert LE, et al. Brachytherapy Training Survey of Radiation Oncology Residents. Int J Radiat Oncol Biol Phys. 2019;103(3):557–560. doi:10.1016/j.ijrobp.2018.10.023 [PubMed: 30612963]
5. Filippou V, Tsoumpas C. Recent advances on the development of phantoms using 3D printing for imaging with CT, MRI, PET, SPECT, and ultrasound. Med Phys. 2018. doi:10.1002/mp.13058
6. Lee Ventola CMedical applications for 3D printing: Current and projected uses. P T. 2014.
7. Schubert C, Van Langeveld MC, Donoso LA. Innovations in 3D printing: A 3D overview from optics to organs. Br J Ophthalmol. 2014. doi:10.1136/bjophthalmol-2013-304446
8. Banks JAdding value in additive manufacturing: Researchers in the United Kingdom and Europe look to 3D printing for customization. IEEE Pulse. 2013. doi:10.1109/MPUL.2013.2279617
9. Cunha JAM, Flynn R, Bélanger C, et al. Brachytherapy Future Directions. Semin Radiat Oncol. 2020. doi:10.1016/j.semradonc.2019.09.001
10. Jones EL, Tonino Baldion A, Thomas C, et al. Introduction of novel 3D-printed superficial applicators for high-dose-rate skin brachytherapy. Brachytherapy. 2017. doi:10.1016/j.brachy.2016.11.003
11. Nattagh K, Siauw T, Pouliot J, Hsu IC, Cunha JA. A training phantom for ultrasound-guided needle insertion and suturing. Brachytherapy. 2014. doi:10.1016/j.brachy.2014.01.003
12. Haie-Meder C, Pötter R, Van Limbergen E, et al. Recommendations from Gynaecological (GYN) GEC-ESTRO Working Group (I): Concepts and terms in 3D image based 3D treatment planning in cervix cancer brachytherapy with emphasis on MRI assessment of GTV and CTV. Radiother Oncol. 2005. doi:10.1016/j.radonc.2004.12.015
13. Viswanathan AN, Thomadsen B. American Brachytherapy Society consensus guidelines for locally advanced carcinoma of the cervix. Part I: General principles. Brachytherapy. 2012. doi:10.1016/j.brachy.2011.07.003
14. Dumane VA, Yuan Y, Sheu RD, Gupta V. Computed tomography-based treatment planning for high-dose-rate brachytherapy using the tandem and ring applicator: Influence of applicator choice on organ dose and inter-fraction adaptive planning. J Contemp Brachytherapy. 2017. doi:10.5114/jcb.2017.68519
15. KleenSpec ® 590 Series Vaginal Speculum Specifications. https://www.welchallyn.com/content/dam/welchallyn/documents/upload-docs/Product-Literature/Specification-Sheet/KleenSpec-590-Vag-Spec-Specifications.pdf.
16. Brandan ME, Fantuzzi E, Gregoire V, Howell RW, Paretzke HG. ICRU Report 89. J ICRU. 2013;13(1):260. https://conferences.iaea.org/indico/event/142/session/10/contribution/8/material/0/2.pdf.
17. Qi HJ, Joyce K, Boyce MC. Durometer hardness and the stress-strain behavior of elastomeric materials. Rubber Chem Technol. 2003. doi:10.5254/1.3547752
18. Methtananda IM, Parker S, Patel MP, Braden M. The relationship between Shore hardness of elastomeric dental materials and Young's modulus. Dent Mater. 2009;25(8):956–959. doi:10.1016/j.dental.2009.02.001 [PubMed: 19286248]
19. Gent AN. On the Relation between Indentation Hardness and Young's Modulus. Rubber Chem Technol. 1958;31(4):896–906. doi:10.5254/1.3542351

20. Baah-Dwomoh A, McGuire J, Tan T, De Vita R. Mechanical Properties of Female Reproductive Organs and Supporting Connective Tissues: A Review of the Current State of Knowledge. Appl Mech Rev. 2016;68(6). doi:10.1115/1.4034442

21. Siddiqui A, Braden M, Patel MP, Parker S. An experimental and theoretical study of the effect of sample thickness on the Shore hardness of elastomers. Dent Mater. 2010. doi:10.1016/j.dental.2010.02.004

22. Milani G, Milani F. AISC 256 - Behavior of Elastomeric Seismic Isolators Varying Rubber Material and Pad Thickness: A Numerical Insight. 2014;256:55. doi:10.1007/978-3-319-03581-9_4

23. Christensen MB, Oberg K, Wolchok JC. Tensile properties of the rectal and sigmoid colon: a comparative analysis of human and porcine tissue. Springerplus. 2015. doi:10.1186/s40064-015-0922-x

24. Li C, Guan G, Zhang F, et al. Quantitative elasticity measurement of urinary bladder wall using laser-induced surface acoustic waves. Biomed Opt Express. 2014. doi:10.1364/boe.5.004313

25. Zhao X, Zhong Y, Ye T, Wang D, Mao B. Discrimination Between Cervical Cancer Cells and Normal Cervical Cells Based on Longitudinal Elasticity Using Atomic Force Microscopy. Nanoscale Res Lett. 2015. doi:10.1186/s11671-015-1174-y

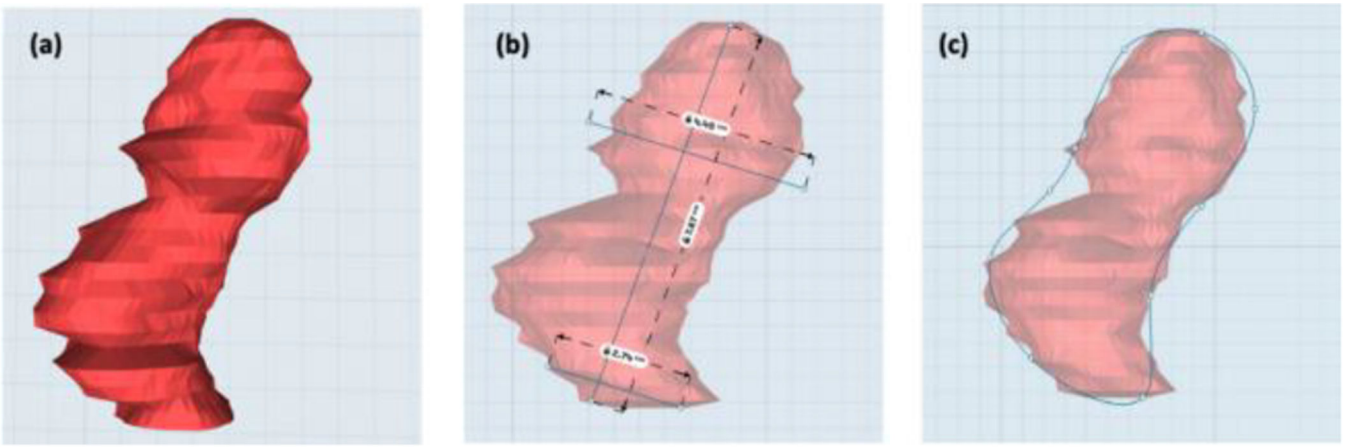

Figure 1.

(a) 3D STL file of uterus with interpolated contour inconsistencies. (b) Average uterus dimensions from patient study sketched around STL file from patient contour. (c) Sketches connected to create smoothened uterus outline.

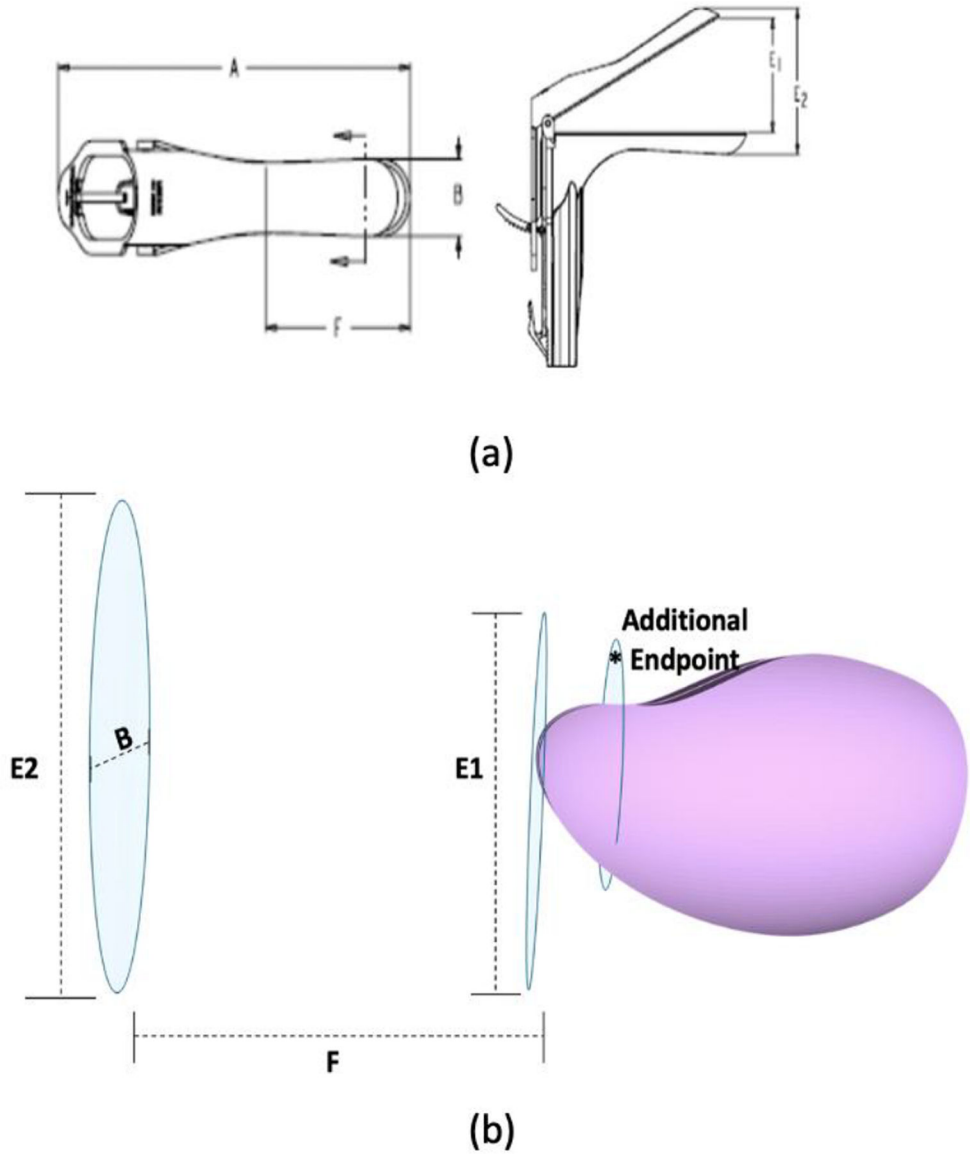

Figure 2:

(a) Dimensions specification diagram for KleenSpec® 590 series vaginal speculum. (b) Sketches used to construct vaginal canal based on speculum dimensions. The additional ellipse encompassing the uterus acts as an endpoint to allow the vaginal canal to collapse down to the height of the uterus.

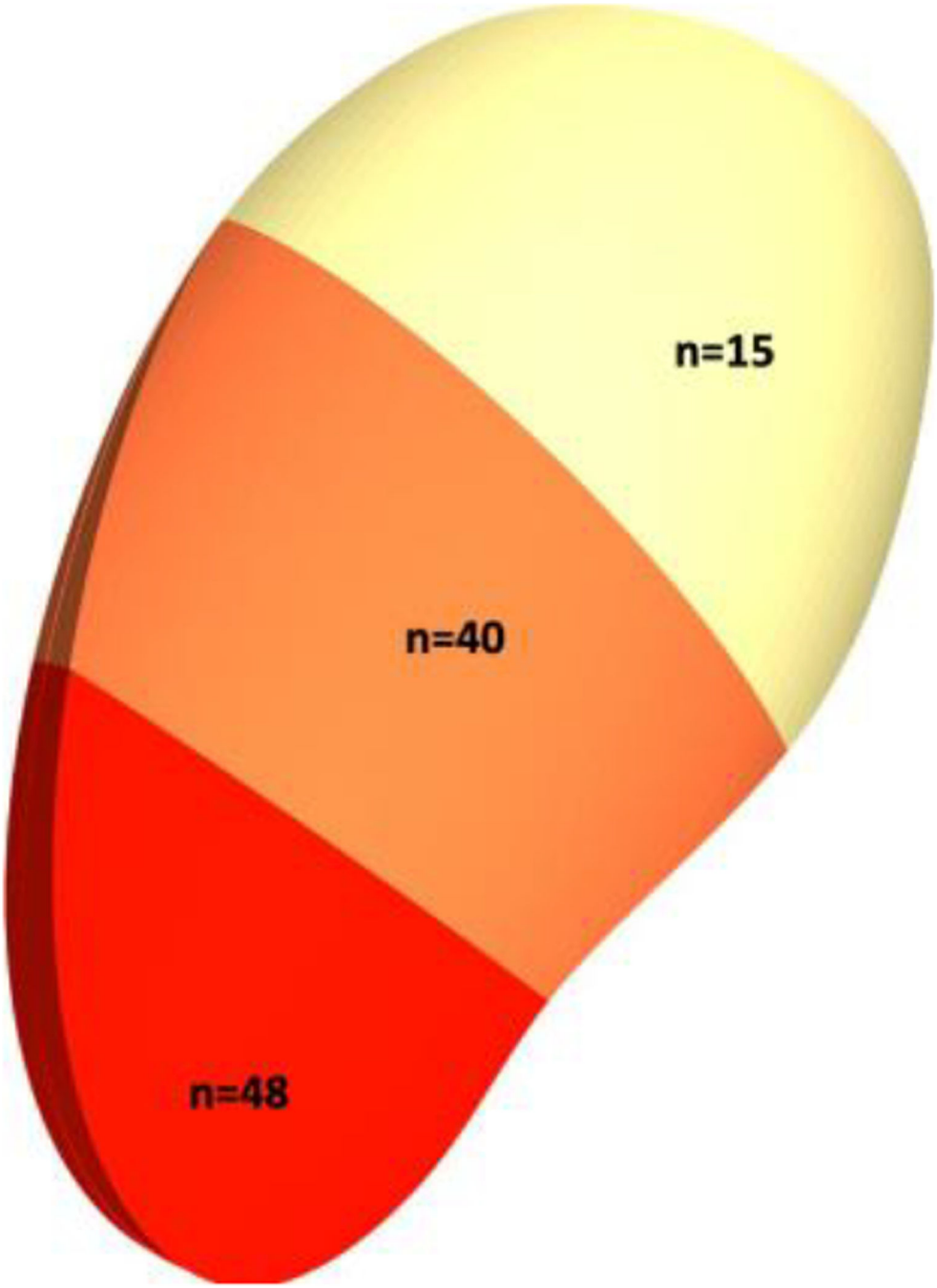

Figure 3:
Occurrences of HR-CTVs occupying specific regions of the uterus from patient study.

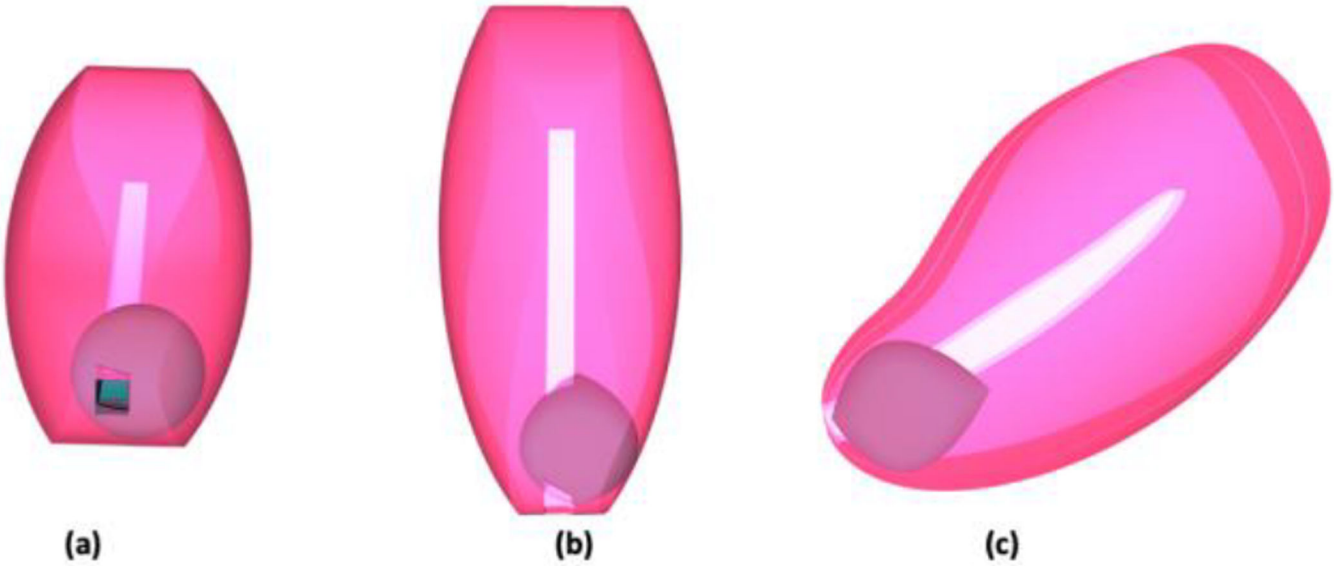

Figure 4:
An internal GTV structure designed using the smallest volume from the HR-CTV volume study and placed inside of uterine body. (a) frontal view, (b) overhead view, (c) lateral view.

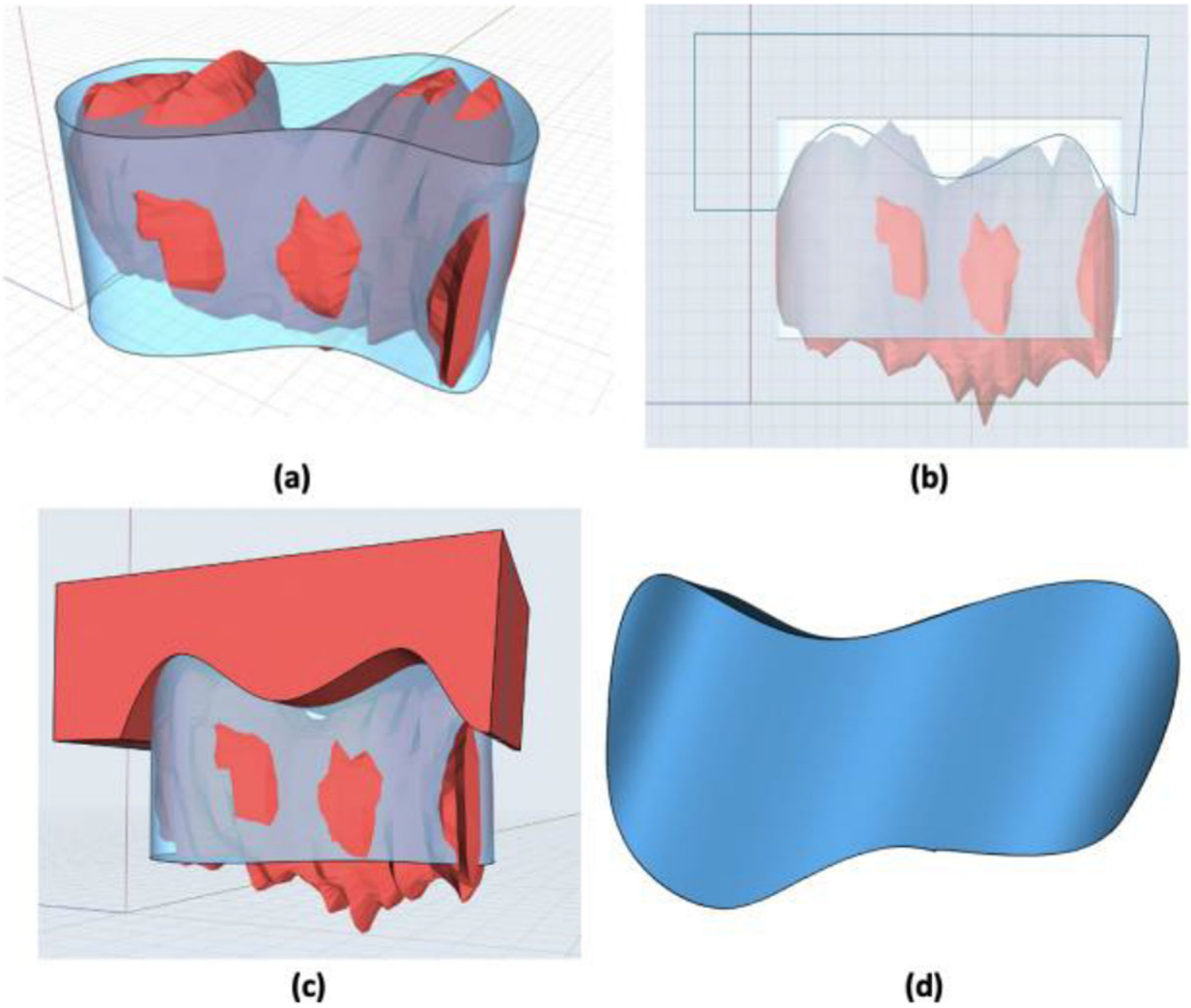

Figure 5:
(a) 2d sketch extracted into 3d body (blue) over the existent uterine body STL file (red). (b) Lateral sketch for Boolean operation. (c) Lateral sketch extracted through uterine body for Boolean subtraction. (d) Uterine body after Boolean subtraction.

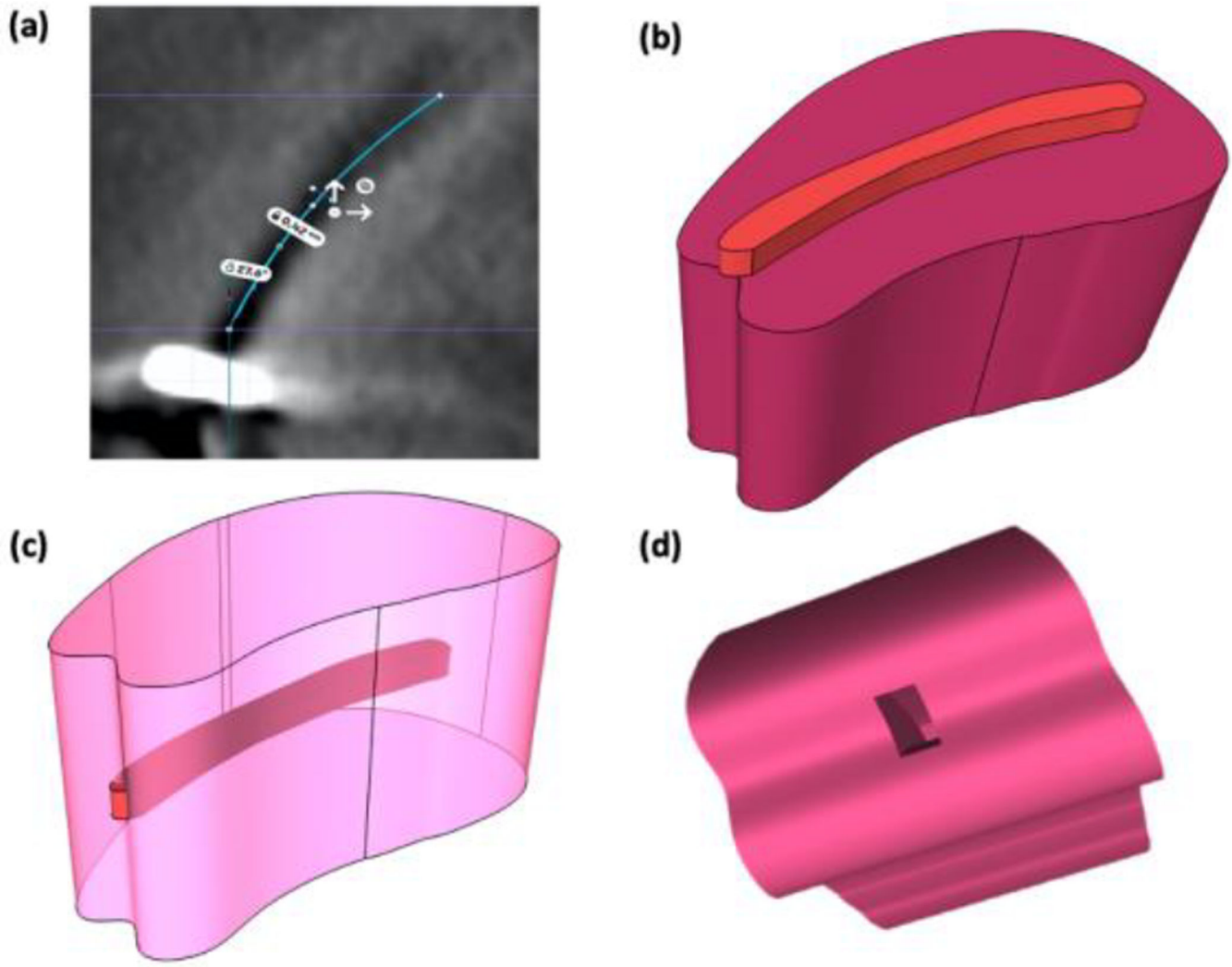

Figure 6:
(a) Dimensions of uterine canal length, width, and angle sketched as measured on the CT image of the uterine canal. (b) Uterine canal sketch extracted and sitting on top of the uterine body. (c) Uterine canal placed in center of the uterine body. (d) Uterine body post Boolean subtraction.

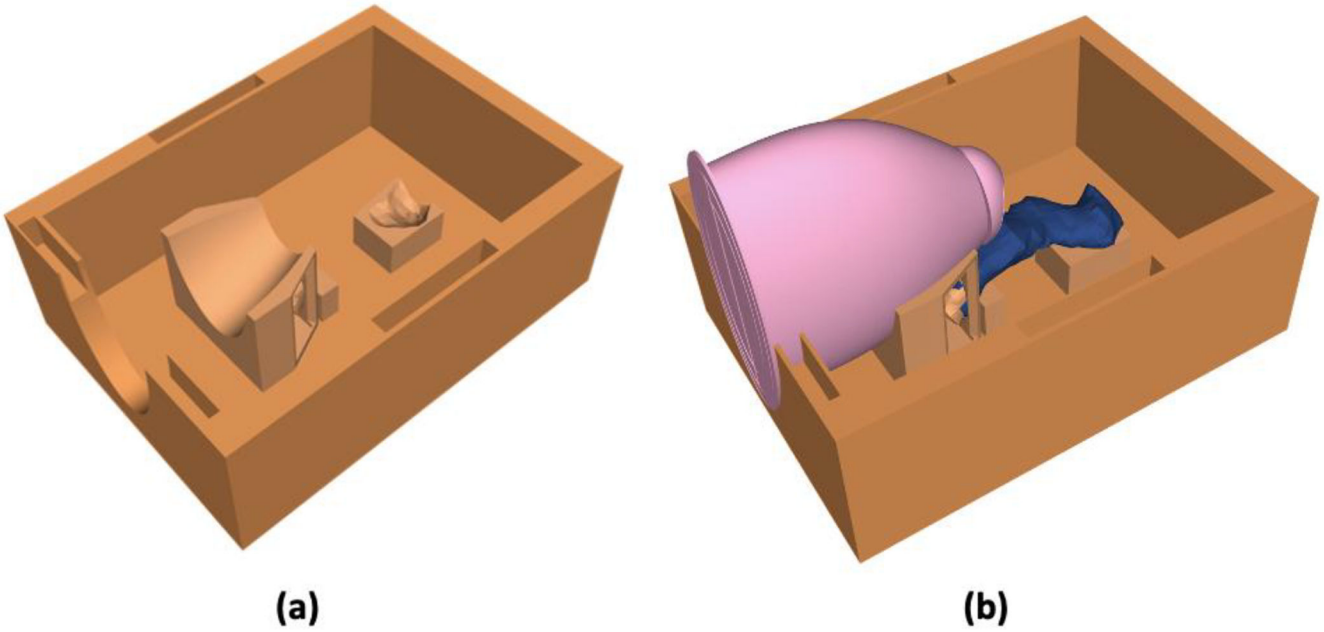

Figure 7:
(a) Vagina and rectum supports integrated into the design of the box. (b) The vagina (pink) and rectum (blue) resting in supports.

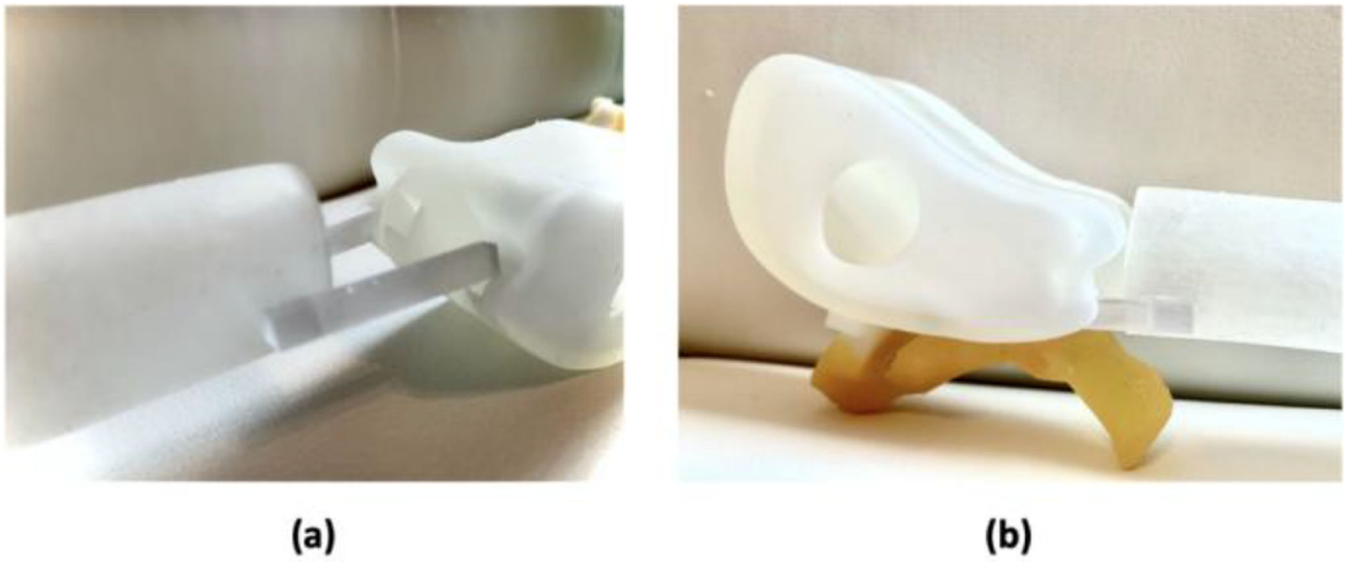

Figure 8:
(a) Pegs attached to vagina at the base of the cavities on the uterine body. (b) Connections of the rectum, uterine body, and vagina through the peg method.

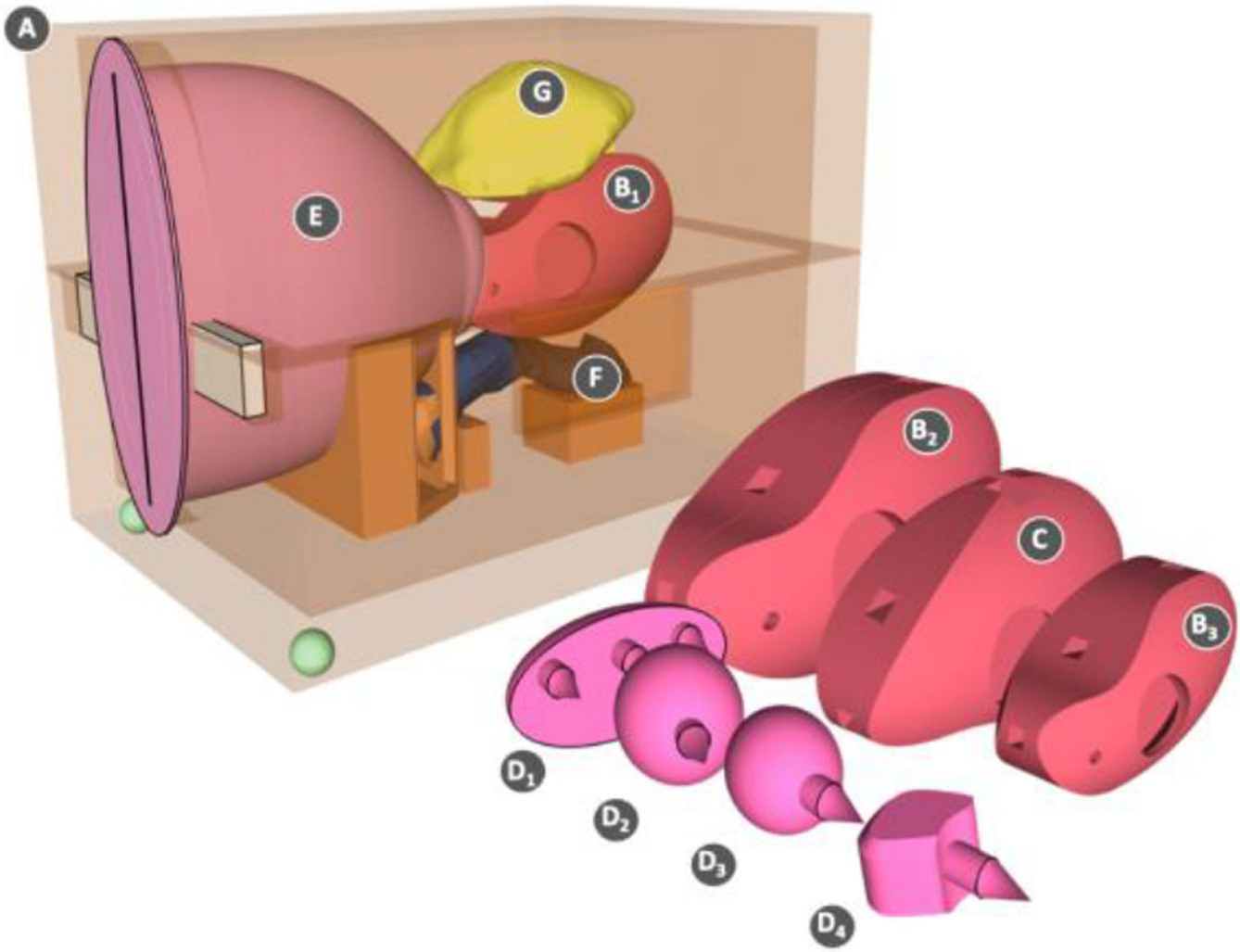

Figure 9:
Full CAD prototype design.

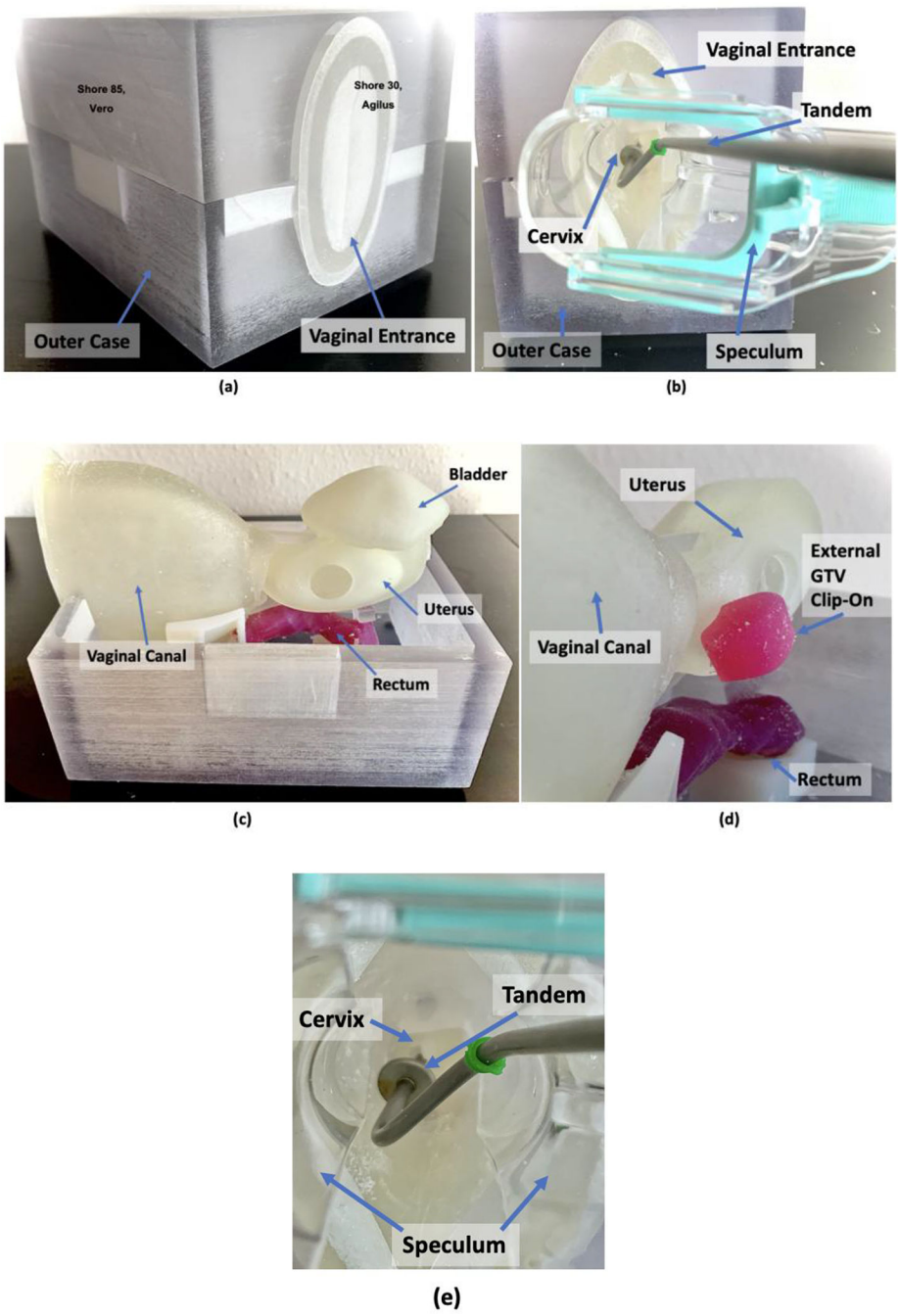

Figure 10:

(A) Closed phantom setup. (b) Speculum entering vaginal canal. (c) 3D printed bottom outer case holding modular organs of interest. (d) Attachment of external GTV clipped into side of uterine body. (e) Tandem fed through speculum and placed inside the cervix and uterine canal.

TABLE 1:

HR-CTV VOLUME RESULTS

	Mean	Minimum	Maximum	Median
HR-CTV Volumes	29.1 ml	5.7 ml	112 ml	22.5

TABLE 2:

UTERUS CONSTRUCTION DIMENSIONS

	U1	U2	U3	U4 *
Body Length	5.81 cm	7.87 cm	9.93	7.87 cm
Body Width (top of cervix)	2.02 cm	2.74 cm	3.45 cm	2.74 cm
Body Width (midpoint)	3.15 cm	4.45 cm	5.74 cm	4.45 cm
Canal Length	5.81 cm	6.23 cm	7.63 cm	6.23 cm
Canal Width	0.34	0.42	0.50	0.42
Canal Angle	19.1°	27.6°	36.1°	27.6°

* Retroverted Uterus

TABLE 3:

ELASTICITY PROPERTIES

	Young's Modulus (MPa)	Calculated Shore A Value
Uterus[20]	0.02 – 1.4	31.3
Vagina[20]	2.5–30	52.37
Rectum[23]	5.18	69.48
Bladder[24]	0.004–0.26	18.17
Cervical Malignancies[25]	0.0012–0.00132	1.37

TABLE 4:

VAGINAL CANAL DIMENSIONS

	Dimension (cm)
Vaginal Canal Length	7.85
Vaginal Entrance Height	7.67
Vaginal End Height	6.07
Vaginal Canal Width	3.25
Vaginal Canal Wall Thickness	.6

TABLE 5:

MATERIAL PROPERTIES ASSIGNED TO PRINTS.

	Photopolymer	Shore A Value
Uterus	Agilus	30
Vagina	Agilus	30
Rectum	Agilus/Vero	70
Bladder	Agilus	30
HR-CTV	Agilus	35
Outer Box	Vero Clear	85
Box Grips	Agilus/Vero	40
Inner Box Supports	Agilus/Vero	50
Modular Connections	Vero Clear	85